Published in final edited form as:
J Neuroimmune Pharmacol. 2014 June ; 9(3): 354–368. doi:10.1007/s11481-014-9524-6.

Repeated Cocaine Treatment Enhances HIV-1 Tat-induced Cortical Excitability *via* Over-activation of L-type Calcium Channels

T. Celeste Napier,
Departments of Pharmacology and Psychiatry, Center for Compulsive Behavior and Addiction, Rush University Medical Center, 1735W. Harrison Street, Cohn Research Building, Rm. 424, Chicago, IL 60612, USA

Lihua Chen,
Department of Pharmacology, Center for Compulsive Behavior and Addiction, Rush University Medical Center, 1735 W. Harrison Street, Cohn Research Building, Rm. 414, Chicago, IL 60612, USA

Fatah Kashanchi, and
National Center for Biodefense and Infectious Diseases, George Mason University, Discovery Hall, Room 306, 10900 University, Blvd. MS 1H8, Manassas, VA 20110, USA

Xiu-Ti Hu
Department of Pharmacology, Center for Compulsive Behavior and Addiction, Rush University Medical Center, 1735 W. Harrison Street, Cohn Research Building, Rm. 414, Chicago, IL 60612, USA

Xiu-Ti Hu: xiu-ti_hu@rush.edu

Abstract

The prefrontal cortex (PFC) is dysregulated in neuroAIDS and during cocaine abuse. Repeated cocaine treatment upregulates voltage gated L-type Ca^{2+} channels in pyramidal neurons within the rat medial PFC (mPFC). L-type Ca^{2+} channels are also upregulated by the HIV-1 neurotoxic protein, Tat, but the role of Tat in pyramidal cell function is unknown. This represents a major knowledge gap as PFC pyramidal neurons are important mediators of behaviors that are disrupted in neuroAIDS and by chronic cocaine exposure. To determine if L-channel-mediated Ca^{2+} dysregulation in mPFC pyramidal neurons are a common neuropathogenic site for Tat and chronic cocaine, we evaluated the electrophysiological effects of recombinant Tat on these neurons in forebrain slices taken from rats 3 days after five, once-daily treatments of cocaine (15 mg/kg, ip) or saline. In saline-treated rats, bath-applied Tat facilitated membrane depolarization and firing. Ca^{2+} influx was increased (indicated by prolonged Ca^{2+} spikes) with low concentrations of Tat (10–40nM), but reduced by higher concentrations (80–160nM), the latter likely reflecting

Correspondence to: Xiu-Ti Hu, xiu-ti_hu@rush.edu.
Drs. Napier and Chen made equal contributions to this project.
Conflict of Interest There is no conflict of interest for any of the authors in this study.

dysfunction associated with excessive excitation. Tat-mediated effects were detected during NMDA/AMPA receptor blockade, and abolished by blocking activated L-channels with diltiazem. In neurons from cocaine-treated rats, the Tat-induced effects on evoked firing and Ca^{2+} spikes were significantly enhanced above that obtained with Tat in slices from saline-treated rats. Thus, glutamatergic receptor-independent over-activation of L-channels contributed to the Tat-induced hyper-reactivity of mPFC pyramidal neurons to excitatory stimuli, which was exacerbated in rats repeatedly exposed to cocaine. Such effects may contribute to the exaggerated neuropathology reported for HIV^+ cocaine-abusing individuals.

Keywords

NeuroAIDS; HIV-1 protein; Pyramidal neuron; Medial prefrontal cortex; Neurotoxicity; Neuropathophysiology

Introduction

Human immunodeficiency virus type 1 (HIV-1)-infected leukocytes invade the central nervous system and secrete HIV-1 proteins that are involved in the pathogenesis of neuroAIDS. NeuroAIDS is characterized by neurocognitive impairments, emotional disturbance, and motor dysfunction (Antinori et al. 2007). NeuroAIDS is more severe and rapidly evolving in cocaine-abusing, HIV^+ individuals than non-abusing, HIV^+ individuals (Nath 2010). The mechanisms that underlie the enhanced neuropathology in the comorbid condition are unclear.

One neurotoxic HIV-1 protein is Tat. Tat is taken up by neurons, and in the nucleus, Tat is transcriptional activator (Li et al. 2009); in the cytoplasm, Tat activates various kinases to promote oxidative stress (Pocernich et al. 2005). Extracellular Tat also has robust effects, e.g., acute, *in vitro* applications of moderate concentrations of Tat (10 nM) activate neurons (Brailoiu et al. 2008), but extended exposure to high concentrations (125–500 nM) cause neuronal damage and death (Nath et al. 2000). These actions are linked to excessive $Ca2^+$ influx mediated in part by ionotropic glutamatergic receptors and the voltage-gated Ca^{2+} channels (Bonavia et al. 2001), for review, see (Haughey and Mattson 2002). Voltage-gated Ca^{2+} channels include the low voltage-activated (LVA) and high voltage-activated (HVA) subfamilies (Catterall et al. 2003; Lipscombe 2002). The LVA-Ca^{2+} channels allow Ca^{2+} entering neurons to depolarize the membrane potential (V_m) and promote activation of HVA-channels. There are several HVA-subtypes, and somatic L-type channels have a critical role in regulating Ca^{2+}-dependent enzymes and gene expression that are important for cell viability (Dolmetsch et al. 2001). We have demonstrated that a functional upregulation of L-type Ca^{2+} channels occurs in medial prefrontal cortex (mPFC) pyramidal neurons following chronic exposure to cocaine (Nasif et al. 2005a,b; Ford et al. 2009). We also have shown that L-channel protein is increased in pyramidal-shaped mPFC neurons 14 days after a Tat injection into the lateral ventricle of rats (Wayman et al. 2012). Pyramidal neurons comprise 80–90 % of neurons in the mPFC, contain glutamate as a neurotransmitter, express ionotropic glutamatergic receptors, and provide a primary excitatory drive for downstream striatal structures (Yuste 2005; Hayton et al. 2010;

Gorelova and Yang 1997). It is well-known that both cocaine and HIV-1 proteins can disrupt to cortical-striatal systems (Nath 2010). This background led to our hypothesis that the L-channels in mPFC pyramidal neurons may be a common target for dysregulation of Ca^{2+} homeostasis by cocaine and Tat. To test this hypothesis, we evaluated the acute effects of Tat on activity of mPFC pyramidal neurons taken from rats repeatedly treated with cocaine. Whole-cell patch-clamp recordings were used to determine if Tat altered firing and Ca^{2+} influx *via* the LVA-/HVA-L-channels, and if Tat-induced effects were independent of ionotropic glutamatergic receptors and enhanced by repeated cocaine exposure.

Materials and Methods

Animals and Treatments

Adolescent male Sprague Dawley rats (Harlan Laboratory, Indianapolis, IN) weighing 75–110 g (4–5 weeks of age) were group-housed in a temperature-controlled vivarium under a 12 hr light/dark cycle. Food and water were available *ad libitum*. A set of untreated rats were used for pilot studies to determine control electrophysiological conditions. For the remaining studies, the rats were administered saline (SAL, 0.1 ml/kg, i.p.) or cocaine (COC, 15 mg/kg, i.p.) once daily for 5 consecutive days followed by 3 days without treatment. This cocaine administration protocol and drug-free time period was selected as our prior work with similarly treated rats verified that it coincides with an enhancement of mPFC pyramidal cell firing (Nasif et al. 2005a, b). All experimental procedures were conducted in accordance with the National Research Council *Guide for the Care and Use of Laboratory Animals* (NIH Publication N.85–23 1996) and were approved by the Institutional Animal Care and Use Committee of Rush University.

Whole-cell Patch-clamp Recording in Brain Slices

Rats were anesthetized with chloral hydrate (400 mg/kg, i.p.) and the brains were immediately excised and immersed in ice-cold, low Ca^{2+}, solution consisting of (in mM): 248 sucrose, 2.9 KCl, 2 $MgSO_4$, 1.25NaH_2PO_4, 10 glucose, 26 $NaHCO_3$, and 0.1 $CaCl_2$; pH 7.4–7.45, with 335–345 mOsm. Three bilateral, 300 μm thick coronal sections, within 2.20 to 3.20 mm anterior to bregma, (according to Paxinos and Watson 1998) were sliced in an oxygenated (95 % O_2/5 % CO_2), low Ca^{2+}, cutting solution. This provided six mPFC-containing hemispheres per rat. The slices were transferred to a holding chamber containing artificial cerebrospinal fluid (aCSF; in mM): 125 NaCl, 2.5 KCl, 25 $NaHCO_3$, 1.25 NaH_2PO_4, 1 $MgCl_2$, 2 $CaCl_2$, and 15 glucose; pH 7.4–7.45, with 305–315 mOsm. After at least 1 hr incubation at room temperature, brain slices were anchored in a recording chamber and perfused with oxygenated aCSF. Current-clamp recordings were performed at ~34 °C. Recording microelectrodes were constructed from glass pipettes pulled with a horizontal pipette puller (p-97 Sutter Instrument Co., Novata, CA) so that the filled electrode had a resistance of 4–6 MΩ. For experiments that monitored evoked action potentials (firing), the electrodes were filled with the following solution (inmM): 120 K-gluconate, 10 HEPES, 0.1 EGTA, 20 KCl, 2 $MgCl_2$, 3 Na_2ATP, and 0.3 NaGTP; pH 7.3–7.35, with 280–285 mOsm. For experiments that monitored voltage-sensitive Ca^{2+} plateau potentials (Ca^{2+} spikes, reflecting Ca^{2+} *influx via* voltage-gated Ca^{2+} channels), the internal solution consisted of (in mM): 140 Cs-gluconate, 10 HEPES, 2 $MgCl_2$, 3 Na_2ATP and 0.3 NaGTP; pH 7.3–7.35,

with 280–285 mOsm. After whole-cell configuration was formed under voltage-clamp recording, this mode was switched to current-clamp for recording of action potentials or Ca^{2+} spikes evoked by membrane depolarization. The signals were amplified and filtered with Axopatch 200B or Multiclamp 700B amplifier (Axon Instruments/ Molecular Devices, Sunnyvale, CA), digitized with Digidata 1322 interface (Axon Instruments), and collected by a PC computer. Whole-cell pipette series resistance was less than 20 MΩ and the bridge was compensated. Na^+-dependent action potentials were generated by 500 ms, depolarizing currents applied in 25 or 50 pA increments. To isolate the voltage-sensitive $Ca2^+$ plateau potentials, Na^+ channels were blocked with tetrodotoxin (TTX, 1 μM; Ascent Scientific) and K^+ channels were blocked with extracellular tetra-ethylammonium (TEA, 20 mM; Sigma) and intracellular Cs-gluconate (140 mM; Sigma)(Hu et al. 2004; Nasif et al. 2005a). In all Ca^{2+} spike experiments, ion channels associated with ionotropic glutamate receptors were blocked with kynurenic acid (2.5 mM; Sigma) and $GABA_A$ receptors were blocked with picrotoxin (100 μM; Sigma) continuously applied in the recording chamber bath.

Recordings were obtained from pyramidal neurons within the layers V-VI of the prelimbic or infralimbic mPFC identified under visual guidance using differential interference contrast-microscopy following our previously published protocols (Nasif et al. 2005a,b; Hu et al. 2004). Recording sites were evenly distributed among the four main treatment groups. Only one neuron was recorded per slice and the number of neurons recorded per rat varied from 1–3. Pyramidal neurons typically exhibit a regular, accommodating firing pattern when electrically stimulated which is readily distinguished from the irregular, burst firing, stuttering, or non-accommodating pattern exhibited by cortical GABAergic interneurons (Markram et al. 2004). For inclusion in study outcomes, recordings from SAL-treated rats, pyramidal neurons had to demonstrate a stable resting membrane potential (RMP) more negative than −63 mV, and a Na^+-dependent action potential amplitude greater than 65 mV. HVA-Ca^{2+} plateau potentials in mPFC pyramidal neurons were evoked by depolarizing currents at relatively high membrane potential levels. These potentials typically exhibit a two-phase ‘plateau’ spike (reflecting Ca^{2+} influx through voltage-gated Ca^{2+} channels mainly from the soma and the proximal dendrites, respectively), with a firing threshold at a membrane potential (V_m) of approximately −20 mV, a duration more than 1000 ms, with an amplitude more than 60 mV. In some neurons, small, subthreshold LVA-Ca^{2+} potentials (‘V_m rebound’) were elicited immediately after hyperpolarizing currents (usually more negative than −110 mV). The LVA-potentials have amplitudes <10 mV above the RMP and do not exhibit the more typical long plateaus. The mean RMP of mPFC pyramidal neurons in this preparation is ~68 mV; therefore, all Ca^{2+} potentials were evoked from a V_m held at this level. This protocol was necessary due to the following: (1) A complete blockade of all types of K^+ channels (by TEA in the bath and cesium in the cytosol) is required to generate a full-sized HVA-Ca^{2+} plateau potential. (2) Blockade of K^+ channels that conduct outward-flowing K^+ currents at the RMP levels drastically depolarizes the RMP (Perez et al. 2011). (3) Standardizing the basal RMP allows for direct comparisons of neuronal responses across the different treatment groups.

For quantification, characteristics of Na^+-dependent action potentials and Ca^{2+} plateau potentials were obtained from the initial spike evoked by the minimal depolarizing current

(rheobase) as measured from the firing threshold. The half-duration was measured at the one-half amplitude level. For evoked Ca^{2+} plateau potentials, the integrated area of LVA- or HVA-Ca^{2+} potentials (mV × ms; which reflects the amount of Ca^{2+} influx *via* voltage-gated Ca^{2+} channels) was measured from the rising part of the potential at the holding/RMP level to the end of the recording episode. The recording episode for Ca^{2+} plateau potentials was 10 s, and the depolarizing current pulse duration was 40 ms. Analysis of other membrane and action potential properties is detailed in our previous studies (Zhang et al. 1998; Hu et al. 2004; Nasif et al. 2005a,b).

Bath Application of Test Compounds

Recombinant HIV-1 Tat (Tat), a 14-kDa protein containing 86–101 amino acids (Contreras et al. 2005), was produced in the laboratory of Dr. Fatah Kashanchi (George Mason University, VA), or provided by NIH AIDS Research and Reference Reagent Program (Germantown, MD). Recombinant Tat is 1,000-fold less potent than that secreted from Tat-expressing cells (Li et al. 2008); therefore, 10–1,000 nM recombinant Tat is thought to approximate Tat concentrations detected in the CSF of HIV-seropositive patients (Westendorp et al. 1995; Xiao et al. 2000; Campbell and Loret 2009). Acute treatment with 10–1,000 nM recombinant Tat facilitates depolarization and spiking in cultured cortical neurons (Bonavia et al. 2001; Brailoiu et al. 2008), and hippocampal pyramidal neurons recorded in rat *ex vivo* brain slices (Cheng et al. 1998; Nath et al. 1996). For the current study, recombinant Tat was evaluated with escalating concentrations of 10, 20, 40, 80 and 160 nM, continuously applied to the recording chamber *via* a recycling system. Our pilot studies with pyramidal neurons showed that continuous, recycled perfusion of a single concentration of Tat produced stable, reproducible effects for the duration of the perfusion, and the magnitude of the effect was similar to that elicited by an equal concentration obtained with the escalating protocol (data not shown). Heat-inactivated Tat (i.e., 40 nM Tat boiled at 85°C for 30 min) was used as a negative control (Avraham et al. 2004; Price et al. 2005). The involvement of L-type Ca^{2+} channels in the Tat-induced effects was verified by response antagonism with diltiazem. Diltiazem (Sigma/RBI, St. Louis, MO) is a selective, high affinity, L-type Ca^{2+} channel blocker (IC_{50}=50.4 nM) (Glossmann et al. 1983) that preferentially blocks activated (open) L-channels (Niimi et al. 2003). Diltiazem was applied in the bath as 10, 20, 40, 80 nM, and 5 μM, with or without co-perfusion of Tat.

Treatment Definitions and Statistical Analysis

Comparisons were made among the following treatment conditions: saline-treated rats (SAL-treated), cocaine-treated rats (COC-treated), basal activity/baseline control (BlCtr, spiking evoked in each pyramidal neuron prior to bath-applied treatments), bath-applied Tat (Tat), and bath-applied diltiazem (Dilt). As an example of the format used to describe the treatment conditions, SAL-Tat/Dilt refers to the brain slices taken from SAL-treated rats wherein recordings of mPFC pyramidal neurons were made during Tat and diltiazem co-perfusion.

Chi-squared test was used for nonparametric comparisons. Student's *t*-test, and one- or two-way repeated measures (rm) ANOVA (including mixed designs) were used to compare membrane properties, characteristics of Na^{+}-dependent action potentials, spiking rate, and

Ca^{2+} plateau potentials. It is noteworthy that the two-way mixed function rmANOVA is based on the assumption that all treatment conditions were independent, although the baseline (BlCtr) and Tat-induced effect measurements were taken from the same cells of either saline (SAL)-treated or cocaine (COC)-treated rats.

Post hoc comparisons were made with Newman-Keuls, Dunnett's tests, or an ANOVA (to ascertain simple main effects). Some data were used in two different comparisons wherein a Bonferroni correction was applied (i.e., $p \leq 0.025$); otherwise, $p \leq 0.05$ was used to denote significance. Data are presented as mean±S.E.M., and *post doc* evaluations are illustrated in the figures denoting $p \leq 0.05$ and $p \leq 0.01$. Statistical analysis was done using SigmoPlot 12 (Systat Software Inc., San Jose, CA) except the *t*-tests which were done using GraphPad Prizm 5 (GraphPad Software Inc., La Jolla, CA).

Results

Effects of Tat on Pyramidal Neurons of Saline-treated Rats

1. Tat increased evoked action potentials and this effect was abolished by diltiazem—In SAL-treated rats (n=17), bath application of 40 nM Tat augmented membrane depolarization-evoked firing in 14 of 22 recorded mPFC pyramidal neurons (63.6 %); two-way rmANOVA; treatment, $F_{(1,13)}=12.489$, $p=0.004$; current, $F_{(7,91)}=312.624$, $p<0.001$; interaction, $F_{(7,91)}=3.898$, $p<0.001$. This effect of Tat is illustrated in Fig. 1A by representative traces from a single neuron, and in Fig. 1B for the 8 neurons (recorded from8 different rats) that were subsequently tested with diltiazem. In contrast, heat-inactivated Tat (40 nM) did not alter evoked firing (n=4 neurons recorded from 2 rats; two-way rmANOVA; treatment, $F_{(1,3)}=0.332$, $p=0.605$; current, $F_{(7,21)}=18.048$, $p<0.001$; interaction, $F_{(7,21)}=0.961$, $p=0.483$) (Fig. 1C).

The involvement of activated L-channels was determined by the ability of diltiazem to abolish Tat-induced excitations. To make this determination, we first conducted a concentration-response analysis of 10–80 nM and 5 μM diltiazem. Diltiazem in 10–80 nM did not significantly alter evoked firing (n=7 neurons from 6 rats; SAL-BlCtr *vs*. SAL-Dilt, two-way rmANOVA; treatment, $F_{(4,24)}=1.060$, $p=0.418$; current, $F_{(7,42)}=24.443$, $p<0.001$; interaction, $F_{(28,168)}=0.979$, $p=0.507$) (Fig. 1D and E), but 5 μM decreased spiking (n=4 neurons from 3 rats; treatment, $F_{(1,3)}=63.563$, $p=0.004$; current, $F_{(7,21)}=58.709$, $p<0.001$; interaction, $F_{(7,\ 21)}=6.584$, $p<0.001$) (see Fig. 1E insert). While 40 nM diltiazem did not significantly alter the number of evoked spikes, paired *t*-test comparisons between SAL-BlCtr and SAL-Dilt (n=7 neurons from 6 rats) revealed that input resistance was increased (130.7±8.9 *vs*. 160.3±13.7 MΩ, respectively; $t_{(6)}=3.619$, $p=0.011$), and the interval measured between the first and second action potential was decreased (10.8±1.6 *vs*. 9.2±1.4 msec, respectively; $t_{(6)}=3.264$, $p=0.017$). Based on these findings, we opted to evaluate the ability of 20 and 40 nM of diltiazem to block the effects of Tat. To do so, we first verified that 40 nM Tat produced a stable response for at least the 20 min time frame needed to perform the antagonism experiments (data not shown). As illustrated in Figs. 1A and B, Tat-induced increases in evoked firing were abolished by co-perfusion of 20–40 nM diltiazem (n=8 neurons from 8 rats; SAL-BlCtr *vs*. SAL-Tat, two-way rmANOVA; treatment, $F_{(2,14)}=8.030$, $p=0.005$; current, $F_{(7,49)}=102.113$, $p<0.001$; interaction, $F_{(14,98)}=2.468$,

p=0.005). Thus, in contrast to the effects of Tat alone, there was no significant difference in spike number between pretreatment basal control and during Tat/diltiazem applications (see Fig. 1B, open circles *vs*. filled squares).

The 40 nM Tat-induced increase in evoked firing was associated with depolarized RMP, increased input resistance (R_{in}), decreased rheobase, and a decrease in the spike amplitude (Table 1). These effects of Tat ceased with wash out (data not shown). Tat did not alter firing threshold, ½ amplitude duration, or after-hyperpolarization (AHP) amplitude (Table 1).

Tat (40 nM) also *decreased* firing in 36 % (n=8/22 neurons; from 8 and 17 rats, respectively) of recorded mPFC pyramidal neurons from SAL-treated rats (Fig. 2A). These cells did not exhibit any other distinguishing characteristics, i.e., without Tat treatment, membrane properties were similar to those showing excitatory responses to Tat. These Tat-induced decreases in firing were associated with more hyperpolarized RMP (SAL-BlCtr *vs*. SAL-Tat, paired *t*-test; $t_{(7)}$=3.987, p=0.005), higher rheobase ($t_{(7)}$=2.497, p=0.041), and reduced spike amplitudes ($t_{(7)}$=4.377, p=0.003) (Fig. 2B–D). These effects were washed out upon removing Tat from the bath (Fig. 2A, lower trace). Other membrane properties were not significantly altered.

2. Tat enhanced LVA-potentials and triggered firing, and L-channel blockade abolished this effect—Under BlCtr conditions, there was only one neuron (n=1/22, 4.5 %; from 1 and 17 rats, respectively) that showed a small potential [‘V_m rebound’, or LVA-potential, that is mediated by the LVA-Ca^{2+} channels (Markram and Sakmann 1994; Lipscombe 2002)], which occurred immediately after a marked membrane *hyperpolarization* (usually more negative than −110 mV), as described previously (Griffith and Matthews 1986; Khateb et al. 1992; Allen et al. 1993). In control conditions, such V_m rebound was negligible or a subthreshold membrane depolarization (Fig. 3A, the upper trace). Tat markedly potentiated this V_m rebound and enlarged the LVA-potential area (Fig. 3A, middle trace; also see Fig. 3B), and this change often triggered spontaneous firing (Fig. 3C). Moreover, after Tat application, significantly more neurons displayed the V_m rebound with firing (n=10/22, 45.5 %; from 10 and 17 rats, respectively; Chi-squared test; $\chi^2_{(1)}$=10.918, p<0.001) (Fig. 3D). The LVA-potentials and spontaneous firing elicited by the potential were observed in the same neurons that showed increased firing to membrane depolarization during Tat perfusion. With two neurons, Tat-induced membrane depolarization led to spontaneous firing even without injection of hyperpolarizing currents, and the frequency of which was markedly increased following the V_m rebound (Fig. 3E).

Tat-induced increase in the LVA V_m rebound (Fig. 3A) and firing (Fig. 3C) were completely blocked by diltiazem (n=9 neurons from 9 rats; one-way rmANOVA; $F_{(2,16)}$=6.743, p=0.008) (Fig. 3B). Thus, the LVA-potential prior to Tat treatment and that obtained during Tat plus diltiazem co-perfusion were nearly identical (see Fig. 3B and C). Although the LVA-Ca^{2+} channels consist of the T-type and L-type channels (Lipscombe 2002) and both types of the channels exist in the rat mPFC cells (Ford et al. 2009), our data support the conclusion that L-channels are the predominate channel that mediate this effect (and the effects of T-channel blockers were not assessed).

3. Tat altered voltage-sensitive Ca^{2+} potentials; diltiazem blocked the effects of low concentrations, but not high concentrations, of Tat—Voltage-sensitive Ca^{2+} influx, reflected by depolarizing current-evoked Ca^{2+} plateau potentials, was assessed in mPFC pyramidal neurons from SAL-treated rats with or without acute Tat perfusion. To do so, TTX-sensitive Na^{+} channels, TEA/cesium-sensitive K^{+} channels, as well as ionotropic glutamatergic and GABAergic receptors were blocked, and HVA-Ca^{2+} plateau potentials were evoked by depolarizing current pulses. To verify the stability of evoked Ca^{2+} plateaus, we used untreated rats and determined that 40 nM Tat enhanced Ca^{2+} plateau potentials that were sustained for at least 25 min (n=3 neurons from 2 rats; one-way rmANOVA of measurements taken every 5 min; $F_{(5,10)}$=5.562, p=0.010). This conclusion was supported by *post hoc* Newman-Keuls evaluations, showing that the maximum effect was achieved after 5 min of perfusing Tat (100±0.0 and 131±10.0 %, for BlCtr and 5 min, respectively; p=0.013), and there was no significant difference in the Ca^{2+} plateau area measured at 5min and 25min post infusion (131±10.0 and 142±12.0 %, respectively; p=0.495).

The recordings provided in Fig. 4A show that 10, 20 and 40 nM Tat prolonged the duration of the Ca^{2+} plateau without altering other characteristics, whereas 80 and 160 nM *decreased* the duration. As illustrated when plateau area is presented as a change from baseline for each concentration of Tat, an asymptote for the plateau enhancement was reached by ~20 nM (Fig. 4B). In three of seven neurons (42.9 %; from 3 and 7 rats, respectively) tested with 160 nM Tat, plateau potentials were reduced, even below that recorded during pretreatment baseline (Fig. 4A and B). These high dose-effects were not reversed even after more than 10 min of perfusing fresh medium(data not shown), which concur with evidence for Tat-induced production of pro-inflammatory cytokines to persist in the brain after Tat is removed (Nath et al. 1999). When exposed to 160 nM Tat, four of the seven neurons (57.1 %) tested demonstrated a pathological profile, wherein the RMP rapidly depolarized (within sec) by at least 10 to 20 mV, and the cell lost its three dimensional structure. These findings demonstrate that Ca^{2+} plateau was increased by low concentrations of Tat, and reduced by high concentrations of Tat, and that high Tat concentrations might even cause damage in some mPFC pyramidal neurons. As recordings were performed with blockade of Na^{+} and K^{+} channels, as well as NMDA/AMPA and $GABA^{A}$ receptors (see Methods), the Tat-induced changes in depolarization-evoked Ca^{2+} potential occurred independent of these modalities. To verify that L-channels mediated these effects, responding during co-perfusion of Tat with the L-channel blocker diltiazem was tested. At 10 nM, diltiazem did not alter the effects of Tat (n=6 cells; data not shown). At 20–40 nM, diltiazem reduced the increases in HVA-Ca^{2+} potentials that occurred with 20–40 nM of Tat (n=6neurons from 6 rats; one-way rmANOVA; $F_{(2,10)}$=8.005, p=0.008; *post-hoc* Newmen-Keuls, p=0.008) (Fig. 4D), without altering evoked Ca^{2+} plateau potentials on its own (Fig. 4C). However, 20–40 nM diltiazam did not antagonize the decreases in plateau duration induced by 80–160 nM Tat; indeed, diltiazem further reduced the duration and amplitude of, or completely suppressed, these Ca^{2+} potentials (n=4 neurons from 4 rats; data not shown). These findings verify that Tat increased voltage-sensitive Ca^{2+} influx predominantly *via* HVA-L-channels, and suggest that the over-activation may be sufficiently excessive to promote a depolarization inactivation and hinder repolarization.

Effect of Tat on Pyramidal Neurons of Cocaine-treated Rats

1. Repeated cocaine increased evoked firing and Tat potentiated this change —Repeated cocaine treatments followed by a 3-day withdrawal increased the number of evoked action potentials by mPFC pyramidal neurons as compared to responses of neurons from SAL-treated rats (e.g., see Fig. 5A). Some neuronal membrane properties were altered in the COC-treated rats (see Table 1); this included a reduced rheobase. These findings concur with our prior demonstration that chronic cocaine increases neuronal excitability (Nasif et al. 2005b).

Tat increased evoked firing in all eleven neurons recorded from five rats with a history of repeated cocaine treatments, the magnitude of which was greater than that seen in the SAL-Tat group (Fig. 5A and B). A mixed factor, two-way rmANOVA among the four treatment conditions (SAL-BlCtr, SAL-Tat, COC-BlCtr, and COC-Tat) showed significant effects for treatment ($F_{(3,38)}$=7.510, p<0.001), current magnitude ($F_{(7,266)}$=297.503, p<0.001), and an interaction ($F_{(21,266)}$=4.485, p<0.001) (Fig. 5B). Significant differences between treatment conditions using a *post-hoc* Newman-Keuls are illustrated in Fig. 5B. SAL-BlCtr and SAL-Tat groups included some cells that were also used to determine the effects of Tat and diltiazem on evoked firing (see Fig. 1B). (It is noted that in contrast to the data presented in Fig.1B, there was no significant difference in the number of spiking evoked by 0.1–0.2 nA currents between SAL-BlCtr and SAL-Tat cells presented in Fig.5B. This outcome difference reflects the differences in statistical analysis used, for in contrast to Fig. 5B, the treatment groups were analysis as dependent events for Fig. 1B.) As shown in Table 1, the membrane properties that were significantly altered with Tat perfusion (COC-Tat) in COC-treated rats included a more depolarized RMP, increased R_{in}, reduced rheobase, increased ½ duration (suggesting enhanced Ca^{2+} influx), and reduced spike amplitude (suggesting interruption of Tat on Na^{+} and/or K^{+} channels). The effects of Tat on decreasing action potential amplitude were also greater in COC-Tat than SAL-Tat.

2. Hyperpolarization-elicited V_m rebound and associated firing was not detected in neurons from cocaine-treated rats—There was no significant difference in the basal occurrence frequency of hyperpolarization-elicited V_m rebound (i.e., LVA-potential) or spontaneous firing in mPFC pyramidal neurons from COC-treated rats as compared to SAL-treated rats. Unlike the responses obtained in SAL-treated rats, Tat did not alter the LVA-potentials or elicit spontaneous firing in pyramidal neurons from COC-treated rats (data not shown).

3. Repeated cocaine increased the duration of Ca^{2+} plateau potentials and Tat prolonged these potentials—Pyramidal neurons from COC-treated rats showed a robust increase in the duration of Ca^{2+} plateau potentials (reflecting an increase in voltage-sensitive Ca^{2+} influx) as compared to those recorded from SAL-treated rats (Fig. 6), as we demonstrated previously (Nasif et al. 2005a). There also was a significant difference in the rheobase between the treatment group baselines (SAL-BlCtr and COC-BlCtr, 0.48±0.01 nA (n=8 neurons from 8 rats) and 0.17±0.01 nA (n=9 neurons from 6 rats), respectively; Student's *t*-test; $t_{(15)}$=3.368, p=0.004). Other characteristics of the HVA-Ca^{2+} plateau potentials were not significantly altered. Bath-applied Tat (1o nM) produced an additional

increase in the Ca^{2+} influx. This phenomenon is illustrated by individual traces showing an exaggerated prolongation of the Ca^{2+} potential duration in neurons from COC-treated rats (Fig. 6A), and by analyzing changes in the area of the Ca^{2+} potential plateau (mV × ms). For plateau area, a two-way rmANOVA revealed a significant difference for treatment ($F_{(1,15)}$=8.016, p=0.013), Tat concentration ($F_{(3,45)}$=8.923, p<0.001), and an interaction ($F_{(3,45)}$=5.112, p=0.004). A *post hoc* Newman-Keuls indicated significant differences between SAL-treated and COC-treated groups at baseline and with 10–40 nM Tat (see Fig. 6B). To assess the effects of Tat concentration within each chronic treatment groups, a simple main effect analysis (one-way rmANOVA) with *post hoc* Dunnett's was used. In neurons from SAL-treated rats, bath-applied Tat (i.e., SAL-Tat) significantly increased the Ca^{2+} potential area at 20 and 40 nM ($F_{(3,21)}$=5.518, p=0.006; Dunnett's, compared to SAL-BlCtr, p<0.01) (Fig. 6B). In neurons from COC-treated rats, the Ca^{2+} potential area reached its maximum level by 10 nM Tat ($F_{(3,24)}$=7.990, p<0.001; Dunnett's, compared to COC-BlCtr, p<0.01). These Tat-induced effects were lost by 40 nM (COC-Tat (40 nM) *vs*. COC-BlCtr; Dunnett's, p=0.143). Thus, in neurons from COC-treated rats, the Ca^{2+} potential area was augmented by 10 and 20 nM Tat, and was reduced by 40 nM, so as to no longer be significantly different from pretreatment baseline (Fig. 6B). These response features are consistent with response blunting per 'overactivation'; therefore, to avoid possible damage induced by over-excitation, concentrations of Tat higher than 40 nM were not tested on neurons from COC-treated rats. This profile contrasted Tat-induced effects in SAL-treated rats, where a significant increase in Ca^{2+} plateau potentials occurred with 20 and 40 nM (Fig. 6B), and decreases were not observed until 80 and 160 nM (see Fig. 4B). Treatment group contrasts were also seen with 10 nM Tat for this concentration did not alter Ca^{2+} influx in SAL-treated rats, but was sufficient to enhance Ca^{2+} influx in neurons from COC-treated rats. These results revealed a leftward shift of the Tat concentration- Ca^{2+} potential response relationship for pyramidal neurons from COC-treated rats as compared to that from SAL-treated rats. This profile illustrates the ability of chronic cocaine to augment the effects of acute Tat on Ca^{2+} influx in mPFC pyramidal neurons.

Discussion

The present study revealed that Tat abnormally increased the excitability of rat mPFC pyramidal neurons *via* an excessive enhancement of Ca^{2+} influx through over-activated L-type Ca^{2+} channels; this effect of Tat was potentiated after repeated cocaine treatment. Given that the mPFC is a critical mediator of cognitive function and reward-motivated behavior which is dysregulated during cocaine abuse (Goldstein and Volkow 2011) and neuroAIDS (Ferris et al. 2008), such channelopathy may contribute to the exaggerated neuropathology reported for HIV^{+} individuals who abuse cocaine.

In SAL-treated rats, Tat increased neuronal excitability *via* depolarizing the RMP and facilitating firing. As the amplitude of the evoked action potentials was decreased and firing threshold was not altered by Tat, it is unlikely that such change was mediated by increased Na^{+} channel activity. Rather, Tat-induced increase in neuronal excitability was prevented by the selective L-channel blocker diltiazem (which preferentially blocks activated/open L-type Ca^{2+} channels), implicating activated L-channels as a target for Tat in mPFC pyramidal neurons. These Tat-mediated responses by mPFC pyramidal neurons in *ex vivo* brain slices

from adolescent rats concur with prior reports of Tat-mediated membrane depolarization and enhanced firing by cultured human cortical cells, and hippocampal neurons in brain slices from neonatal rats (Brailoiu et al. 2008; Cheng et al. 1998; Nath et al. 1996). Tat-induced Ca^{2+} influx was demonstrated by a prolongation of HVA-Ca^{2+} spikes (plateau potentials), and this effect could disturb intracellular Ca^{2+} homeostasis and when in excess, dysregulate neuronal function. Ca^{2+} influx *via* the LVA-Ca^{2+} channels, (i.e., those channels which were activated at less depolarized membrane potential levels and were associated with rebound spiking), was also increased by Tat. This effect was also nullified by diltiazem, indicating an involvement of the L-channels activated at low membrane voltages. To the best of our knowledge, the effects of Tat on the LVA-L channels have not been reported; therefore, our findings revealed a previously-unknown mechanism for Tat to alter Ca^{2+} homeostasis. Thus, our findings demonstrate that Tat abnormally increased activity of both HVA- and LVA-L channels and associated spiking in mPFC pyramidal neurons.

Tat can act on a low-density lipoprotein coupled to NMDA receptors to induce Ca^{2+} influx (Liu et al. 2000; Eugenin et al. 2007), and NMDA receptors, like LVA-Ca^{2+} channels, regulate subthreshold excitability of cortical pyramidal neurons (Markram and Sakmann 1994; Markram et al. 1997). The present study provided the first evidence for Tat-induced changes in LVA-Ca^{2+} channels that are *independent* of NMDA receptors, as all recordings were conducted during blockade of ionotropic glutamatergic receptors. Thus, it is likely that Tat dysregulates Ca^{2+} influx independent of, and also *via* actions on NMDA receptors (Bonavia et al. 2001). Both processes can depolarize resting membrane potentials, and can cause over-activation of the HVA-L channel to excessively increase cytosolic Ca^{2+} levels. Such multiplicity of action provides a powerful means for Tat to promote Ca^{2+} influx, and this action can have dire consequences on the plethora of Ca^{2+}-dependent intracellular processes critical for neuronal homeostasis.

We demonstrated that the ability of Tat to prolong Ca^{2+} spikes and facilitating firing were concentration-dependent; lower concentrations of Tat (10–40nM) increased Ca^{2+} influx and excitability, whereas both responses were reduced at higher concentrations (80–160nM). Also with 160nM, 57.1 % of the neurons studied exhibited the signs of severe neuronal damage, and the recordings abated. The lower Tat concentrations (10–40nM) used here are comparable to the levels of Tat detected in the CSF of HIV-1 seropositive patients (Li et al. 2008; Xiao et al. 2000;Westendorp et al. 1995). The reduced-excitatory responses to higher concentrations of Tat (80–160nM) likely reflected neuronal inactivation as a consequence of excessive Ca^{2+} influx and saturation of normal mechanisms for buffering the intracellular Ca^{2+} levels. Moreover, while the electrophysiological methods used here do not allow for a definitive determination, the recordings lost *w*ith 160nMTatmay have reflected Tat-induced excitotoxicity that was extreme enough to cause severe damage or even death of the recorded pyramidal neuron. Such a profile may occur inHIV^{+} individuals, wherein during early exposure and/or with lower brain Tat levels, mPFC pyramidal neurons may become over-activated, but due to the normal capacity of the neurons to compensate, a functional dysregulation may be the extent of the neuropathology. However, with over-activation, either with high concentrations of Tat, or long-term exposure to the protein, these buffering mechanisms become exhausted, so that more sever pathophysiology could ensure.

Repeated cocaine treatments increased the reactivity of mPFC pyramidal neurons to excitatory stimuli, and potentiated the effects of Tat on these cells. For example, a subthreshold concentration of Tat that did not alter responses of mPFC pyramidal neurons from SAL-treated rats, was sufficient to enhance Ca^{2+} influx for the neurons from COC-treated rats. The statistically significant interaction indicates that cocaine *potentiated* the effects of Tat, i.e., the action was greater than simple additivity. This outcome suggests that the aberrant plasticity engaged by chronic cocaine exposure, and the acute actions of Tat, converge on the L-channel *via* separate pathways (at least in part). While the literature is sparse on the topic, there is mounting evidence that provides insight into probable mechanisms which differentiate the consequences of chronic cocaine and acute Tat. Examples include the following: We have previously demonstrated that chronic cocaine upregulates L-channel proteins (Ford et al. 2009), and we show here that within the time frame of the electrophysiological studies, responding of acute Tat was stable and therefore did not reflect an increase in channel number. In the mPFC, chronic cocaine is known to upregulate D1 dopamine receptor-mediated cascades that involve enhancing protein kinase A which phosphorylates L-channels, and in so doing, enhances channel conduction (for review, see Hu 2007). This pathway is not known to be activated by Tat, but future studies are needed to validate if it is indeed independent of Tat-induced effects. It is known that Tat has several functional domains, and an emerging literature is identifying various potential binding sites on the cytoplasmic surface of cells (for review, see Bonavia et al. 2001; Haughey and Mattson 2002) that may provide unique means to alter L-channel function. Some Tat-binding sites (e.g., the low density lipoprotein receptor-related protein; LRP) serve to transport extracellular Tat inside the cell, but Tat-induced membrane depolarization of neurons appears to be dependent on extracellular (and not intracellular) Ca^{2+} (Cheng et al. 1998). There also is evidence for direct binding of Tat to the L-channels in human natural killer cells (Zocchi et al. 1998). It is noteworthy, that NMDA receptors can be involved in both the neural adaptations mediated by chronic cocaine (Wolf 1998; Stuber et al. 2010), and acute Tat (Haughey et al. 2001; Rumbaugh et al. 2007), but this link was removed in the current study by blocking NMDA receptors. Thus, it is likely that L-channel activation, regulated by NMDA receptors and/or independent of these receptors, plays an important role in the increases of Ca^{2+} influx associated to acute Tat and chronic cocaine. Finally, the current study revealed that not all consequences of L-channel adaptations covary. For example, 40nM Tat failed to induce the V_m rebound and associated spiking in neurons from cocaine-treated rats. Whether this absence reflected a potentiated cocaine/Tat excitotoxicity or a protective compensation requires further investigation.

The finding that Tat potentiated neuronal consequences of repeated cocaine supports a recent demonstration of such interaction in behaving rodents. Using transgenic mice with an inducible Tat gene, McLaughlin and colleagues revealed that cocaine-induced hyperlocomotion and conditioned place preference were enhanced with brain expression of Tat (Paris et al. 2014). Conditioned place preference is an associative learning task that provides an indirect measure of the cocaine-mediated reward. Using this task to model the tendency of drug-withdrawn human addicts to relapse to drug-taking, these authors revealed that induction of Tat was sufficient to reinstate cocaine place preference in mice whose preference was previously extinguished. These exciting behavioral findings demonstrated

that Tat is able to enhance cocaine-mediated reward and to promote cocaine-seeking after withdrawal. As these behaviors drive the continued abuse use of cocaine by human addicts, it may be that neurotoxic HIV-1 proteins like Tat may compromise the capacity of the co-morbid individual to cease their drug use, and in so doing promote a pathology 'spiral' that underpins the exaggerated morbidity and mortality reported for cocaine-abusing HIV^+ individuals (Cohn SE et al. 2011; Tiwari et al. 2013).

Understanding the functional convergence of neuronal consequences of repeated cocaine administration and acute Tat exposure sheds new light on putative biological mechanisms involved with cocaine abuse and HIV^+ co-morbidity. The fact that the PFC was involved is relevant as PFC maladaptations in human cocaine abusers is associated with the enhanced significance of cocaine (Goldstein and Volkow 2011) and mnemonic deficits (Verdejo-Garcia et al. 2006), as well as a cognitive decline in neuroAIDS (Antinori et al. 2007). Determining that mPFC pyramidal neurons were disrupted is relevant as these neurons provide critical glutamatergic drive to subcortical structures (Kalivas and Volkow 2011) that regulate reward, motivation, cognition and motor function, all of which are altered in cocaine-abusing humans (Volkow et al. 2005; Goldstein and Volkow 2011), in those presenting neuroAIDS (Antinori et al. 2007) and in the co-morbid condition (Ferris et al. 2008). The finding that L-type channels, which are upregulated by repeated cocaine administration, were also necessary for the Tat-induced changes in pyramidal neuron excitability provides a novel target for putative pharmacotherapeutic interventions. We revealed that blocking these channels with diltiazem was sufficient to restore neuronal function that was dysregulated by acute exposure to Tat, indicating the potential value of such therapy early after initial infection with HIV. This approach may preempt Tat-induced cell damage (current study) or death (Nath et al. 2000) known to occur with high doses or long-term exposure. Finally, as diltiazem is already FDA-approved for therapy of other human diseases it can be rapidly moved to clinical trials to ascertain its utility in reducing cocaine/HIV-mediated neuropathogenesis in humans.

In summary, this study demonstrates that acute Tat exposure *in vitro* abnormally increases the reactivity of rat mPFC pyramidal neurons to excitatory stimuli by excessively enhancing Ca^{2+} influx *via* over-activated L-channels. The pathophysiological effects of Tat were related to Tat concentrations, where low concentrations significantly dysregulated mPFC neurons without causing damage or cell death, but that overt toxicity ensued with higher concentrations. This study also revealed that chronic cocaine exposure enhanced the effects of Tat on L-type Ca^{2+} channels. Given that proper regulation of Ca^{2+} influx is critical to normal function and viability of neurons, these findings suggest that the L-type Ca^{2+} channel may be a site at which cocaine and Tat synergize to contribute to CNS dysfunction in cocaine-abusing HIV^+ individuals.

Acknowledgments

This study was supported by the National Institute on Drug Abuse (DA026746, DA033882), the Peter F. McManus Charitable Trust, the Daniel and Ada Rice Foundation, the Chicago Developmental Center for AIDS Research (P30AI082151) and the Center for Compulsive Behavior and Addiction at Rush University Medical Center. We thank Dr. Jingli Zhang for his technical contribution, and Drs. Lena Al-Harthi and Steven Graves for their helpful discussions.

References

Allen TGJ, Sim JA, Brown DA. The whole-cell calcium current in acutely dissociated magnocellular cholinergic basal forebrain neurones of the rat. J Physiol Lond. 1993; 460:91–116. [PubMed: 7683720]

Antinori A, et al. Updated research nosology for HIV-associated neurocognitive disorders. Neurology. 2007; 69:1789–1799. [PubMed: 17914061]

Avraham HK, Jiang S, Lee TH, Prakash O, Avraham S. HIV-1 Tat-mediated effects on focal adhesion assembly and permeability in brain microvascular endothelial cells. J Immunol. 2004; 173:6228–6233. [PubMed: 15528360]

Bonavia R, Bajetto A, Barbero S, Albini A, Noonan DM, Schettini G. HIV-1 Tat causes apoptotic death and calcium homeostasis alterations in rat neurons. Biochem Biophys Res Commun. 2001; 288:301–308. [PubMed: 11606043]

Brailoiu GC, Brailoiu E, Chang JK, Dun NJ. Excitatory effects of human immunodeficiency virus 1 Tat on cultured rat cerebral cortical neurons. Neuroscience. 2008; 151:701–710. [PubMed: 18164555]

Campbell GR, Loret EP. What does the structure-function relationship of the HIV-1 Tat protein teach us about developing an AIDS vaccine? Retrovirology. 2009; 6:50. [PubMed: 19467159]

Catterall WA, Striessnig J, Snutch TP, Perez-Reyes E. International Union of Pharmacology. XL. Compendium of voltage-gated ion channels: calcium channels. Pharmacol Rev. 2003; 55:579–581. [PubMed: 14657414]

Cheng J, Nath A, Knudsen B, Hochman S, Geiger JD, Ma M, Magnuson DS. Neuronal excitatory properties of human immunodeficiency virus type 1 Tat protein. Neuroscience. 1998; 82:97–106. [PubMed: 9483506]

Cohn SE, Jiang H, McCutchan JA, Koletar SL, et al. Association of ongoing drug and alcohol use with non-adherence to aniretroviral therapy and higher risk of AIDS and death: results from ACTG 362. AIDS Care. 2011; 23:775–785. [PubMed: 21293986]

Contreras X, Bennasser Y, Chazal N, Moreau M, Leclerc C, Tkaczuk J, Bahraoui E. Human immunodeficiency virus type 1 Tat protein induces an intracellular calcium increase in human monocytes that requires DHP receptors: involvement in TNF-alpha production. Virology. 2005; 332:316–328. [PubMed: 15661163]

Dolmetsch RE, Pajvani U, Fife K, Spotts JM, Greenberg ME. Signaling to the nucleus by an L-type calcium channel-calmodulin complex through the MAP kinase pathway. Science. 2001; 294:333–339. [PubMed: 11598293]

Eugenin EA, King JE, Nath A, Calderon TM, Zukin RS, Bennett MV, Berman JW. HIV-tat induces formation of an LRP-PSD-95-NMDAR-nNOS complex that promotes apoptosis in neurons and astrocytes. Proc Natl Acad Sci U S A. 2007; 104:3438–3443. [PubMed: 17360663]

Ferris MJ, Mactutus CF, Booze RM. Neurotoxic profiles of HIV, psychostimulant drugs of abuse, and their concerted effect on the brain: Current status of dopamine system vulnerability in NeuroAIDS. Neurosci Biobehav Rev. 2008; 32:883–909. [PubMed: 18430470]

Ford KA, Wolf ME, Hu XT. Plasticity of L-type Ca2+ channels after cocaine withdrawal. Synapse. 2009; 63:690–697. [PubMed: 19360908]

Glossmann H, Linn T, Rombusch M, Ferry DR. Temperature-dependent regulation of d-cis-[3H]diltiazem binding to Ca2+ channels by 1,4-dihydropyridine channel agonists and antagonists. FEBS Lett. 1983; 160:226–232. [PubMed: 6309565]

Goldstein RZ, Volkow ND. Dysfunction of the prefrontal cortex in addiction: neuroimaging findings and clinical implications. Nat Rev Neurosci. 2011; 12:652–669. [PubMed: 22011681]

Gorelova N, Yang CR. The course of neural projection from the prefrontal cortex to the nucleus accumbens in the rat. Neuroscience. 1997; 76:689–706. [PubMed: 9135043]

Griffith WH, Matthews RT. Electrophysiology of AChE-positive neurons in basal forebrain slices. Neurosci Lett. 1986; 71:169–174. [PubMed: 3785743]

Haughey NJ, Mattson MP. Calcium dysregulation and neuronal apoptosis by the HIV-1 proteins Tat and gp120. J Acquir Immune Defic Syndr. 2002; 31(Suppl 2):S55–S61. [PubMed: 12394783]

Haughey NJ, Nath A, Mattson MP, Slevin JT, Geiger JD. HIV-1 Tat through phosphorylation of NMDA receptors potentiates glutamate excitotoxicity. J Neurochem. 2001; 78:457–467. [PubMed: 11483648]

Hayton SJ, Lovett-Barron M, Dumont EC, Olmstead MC. Target-specific encoding of response inhibition: increased contribution of AMPA to NMDA receptors at excitatory synapses in the prefrontal cortex. J Neurosci. 2010; 30:11493–11500. [PubMed: 20739571]

Hu X-T. Cocaine withdrawal and neuro-adaptations in ion channel function. Mol Neurobiol. 2007; 35:95–112. [PubMed: 17519508]

Hu X-T, Basu S, White FJ. Repeated cocaine administration suppresses HVA-Ca2+ potentials and enhances activity of K+ channels in rat nucleus accumbens neurons. J Neurophysiol. 2004; 92:1597–1607. [PubMed: 15331648]

Kalivas PW, Volkow ND. New medications for drug addiction hiding in glutamatergic neuroplasticity. Mol Psychiatry. 2011; 16:974–986. [PubMed: 21519339]

Khateb A, Mühlethaler M, Alonso A, Serafin M, Mainville L, Jones BE. Cholinergic nucleus basalis neurons display the capacity for rhythmic bursting activity mediated by low-threshold calcium spikes. Neuroscience. 1992; 51:489–494. [PubMed: 1488109]

Li W, Huang Y, Reid R, Steiner J, Malpica-Llanos T, Darden TA, Shankar SK, Mahadevan A, Satishchandra P, Nath A. NMDA receptor activation by HIV-Tat protein is clade dependent. J Neurosci. 2008; 28:12190–12198. [PubMed: 19020013]

Li W, Li G, Steiner J, Nath A. Role of Tat protein in HIV neuropathogenesis. Neurotox Res. 2009; 16:205–220. [PubMed: 19526283]

Lipscombe D. L-type calcium channels - Highs and new lows. Circ Res. 2002; 90:933–935. [PubMed: 12016257]

Liu Y, Jones M, Hingtgen CM, Bu G, Laribee N, Tanzi RE, Moir RD, Nath A, He JJ. Uptake of HIV-1 tat protein mediated by low-density lipoprotein receptor-related protein disrupts the neuronal metabolic balance of the receptor ligands. Nat Med. 2000; 6:1380–1387. [PubMed: 11100124]

Markram H, Sakmann B. Calcium transients in dendrites of neocortical neurons evoked by single subthreshold excitatory postsynaptic potentials via low-voltage-activated calcium channels. Proc Natl Acad Sci U S A. 1994; 91:5207–5211. [PubMed: 8197208]

Markram H, Lubke J, Frotscher M, Sakmann B. Regulation of synaptic efficacy by coincidence of postsynaptic APs and EPSPs. Science. 1997; 275:213–215. [PubMed: 8985014]

Markram H, Toledo-Rodriguez M, Wang Y, Gupta A, Silberberg G, Wu C. Interneurons of the neocortical inhibitory system. Nat Rev Neurosci. 2004; 5:793–807. [PubMed: 15378039]

Nasif FJ, Hu XT, White FJ. Repeated cocaine administration increases membrane voltage-sensitive calcium currents in response to membrane depolarization in medial prefrontal cortex pyramidal neurons. J Neurosci. 2005a; 25:3674–3679. [PubMed: 15814798]

Nasif FJ, Sidiropoulou K, Hu XT, White FJ. Repeated cocaine administration increases membrane excitability of pyramidal neurons in the rat medial prefrontal cortex. J Pharmacol Exp Ther. 2005b; 312:1305–1313. [PubMed: 15574686]

Nath A. Human immunodeficiency virus-associated neurocognitive disorder: pathophysiology in relation to drug addiction. Ann N Y Acad Sci. 2010; 1187:122–128. [PubMed: 20201849]

Nath A, Psooy K, Martin C, Knudsen B, Magnuson DS, Haughey N, Geiger JD. Identification of a human immunodeficiency virus type 1 Tat epitope that is neuroexcitatory and neurotoxic. J Virol. 1996; 70:1475–1480. [PubMed: 8627665]

Nath A, Conant K, Chen P, Scott C, Major EO. Transient exposure to HIV-1 Tat protein results in cytokine production in macrophages and astrocytes. A hit and run phenomenon. J Biol Chem. 1999; 274:17098–17102. [PubMed: 10358063]

Nath A, Haughey NJ, Jones M, Anderson C, Bell JE, Geiger JD. Synergistic neurotoxicity by human immunodeficiency virus proteins Tat and gp120: protection by memantine. Ann Neurol. 2000; 47:186–194. [PubMed: 10665489]

Niimi Y, Hino N, Ochi R. Diltiazem facilitates inactivation of single L-type calcium channels in guinea pig ventricular myocytes. Jpn Heart J. 2003; 44:1005–1014. [PubMed: 14711194]

Paris JJ, Carey AN, Shay CF, Gomes SM, He JJ, McLaughlin JP. Effects of Conditional Central Expression of HIV-1 Tat Protein to Potentiate Cocaine-Mediated Psychostimulation and Reward Among Male Mice. Neuropsychopharmacology. 2014; 39:380–388. [PubMed: 23945478]

Paxinos, G.; Watson, C. The Rat Brain in Stereotaxic Coordinates. New York: Academic Press; 1998.

Perez MF, Ford KA, Goussakov I, Stutzmann GE, Hu XT. Repeated cocaine exposure decreases dopamine D2-like receptor modulation of Ca(2+) homeostasis in rat nucleus accumbens neurons. Synapse. 2011; 65:168–180. [PubMed: 20665696]

Pocernich CB, Sultana R, Mohmmad-Abdul H, Nath A, Butterfield DA. HIV-dementia, Tat-induced oxidative stress, and antioxidant therapeutic considerations. Brain Res Brain Res Rev. 2005; 50:14–26. [PubMed: 15890409]

Price TO, Ercal N, Nakaoke R, Banks WA. HIV-1 viral proteins gp120 and Tat induce oxidative stress in brain endothelial cells. Brain Res. 2005; 1045:57–63. [PubMed: 15910762]

Rumbaugh JA, Li G, Rothstein J, Nath A. Ceftriaxone protects against the neurotoxicity of human immunodeficiency virus proteins. J Neurovirol. 2007; 13:168–172. [PubMed: 17505985]

Stuber GD, Hopf FW, Tye KM, Chen BT, Bonci A. Neuroplastic alterations in the limbic system following cocaine or alcohol exposure. Curr Top Behav Neurosci. 2010; 3:3–27. [PubMed: 21161748]

The National Research Council. Guide for the Care and Use of Laboratory Animals. 1996 (NIH Publication N. 85-23).

Tiwari S, Nair MP, Saxena SK. Latest trends in drugs of abuse - HIV infection and neuroAIDS. Future Virol. 2013; 8:121–127. [PubMed: 23626655]

Verdejo-Garcia A, Bechara A, Recknor EC, Perez-Garcia M. Executive dysfunction in substance dependent individuals during drug use and abstinence: An examination of the behavioral, cognitive and emotional correlates of addiction. J Int Neuropsychol Soc. 2006; 12:405–415. [PubMed: 16903133]

Volkow ND, Wang GJ, Ma Y, Fowler JS, et al. Activation of orbital and medial prefrontal cortex by methylphenidate in cocaine-addicted subjects but not in controls: relevance to addiction. J Neurosci. 2005; 25:3932–3939. [PubMed: 15829645]

Wayman WN, Dodiya HB, Persons AL, Kashanchi F, Kordower JH, Hu X-T, Napier TC. Enduring cortical alterations after a single in vivo treatment of HIV-1 Tat. Neuroreport. 2012; 23:825–829. [PubMed: 22828409]

Westendorp MO, Frank R, Ochsenbauer C, Stricker K, Dhein J, Walczak H, Debatin KM, Krammer PH. Sensitization of T cells to CD95-mediated apoptosis by HIV-1 Tat and gp120. Nature. 1995; 375:497–500. [PubMed: 7539892]

Wolf ME. The role of excitatory amino acids in behavioral sensitization to psychomotor stimulants. Prog Neurobiol. 1998; 54:679–720. [PubMed: 9560846]

Xiao H, Neuveut C, Tiffany HL, Benkirane M, Rich EA, Murphy PM, Jeang KT. Selective CXCR4 antagonism by Tat: implications for in vivo expansion of coreceptor use by HIV-1. Proc Natl Acad Sci U S A. 2000; 97:11466–11471. [PubMed: 11027346]

Yuste R. Origin and classification of neocortical interneurons. Neuron. 2005; 48:524–527. [PubMed: 16301166]

Zhang X-F, Hu X-T, White FJ. Whole-cell plasticity in cocaine withdrawal:reduced sodium currents in nucleus accumbens neurons. J Neuroscience. 1998; 18:488–498.

Zocchi MR, Rubartelli A, Morgavi P, Poggi A. HIV-1 Tat inhibits human natural killer cell function by blocking L-type calcium channels. J Immunol. 1998; 161:2938–2943. [PubMed: 9743356]

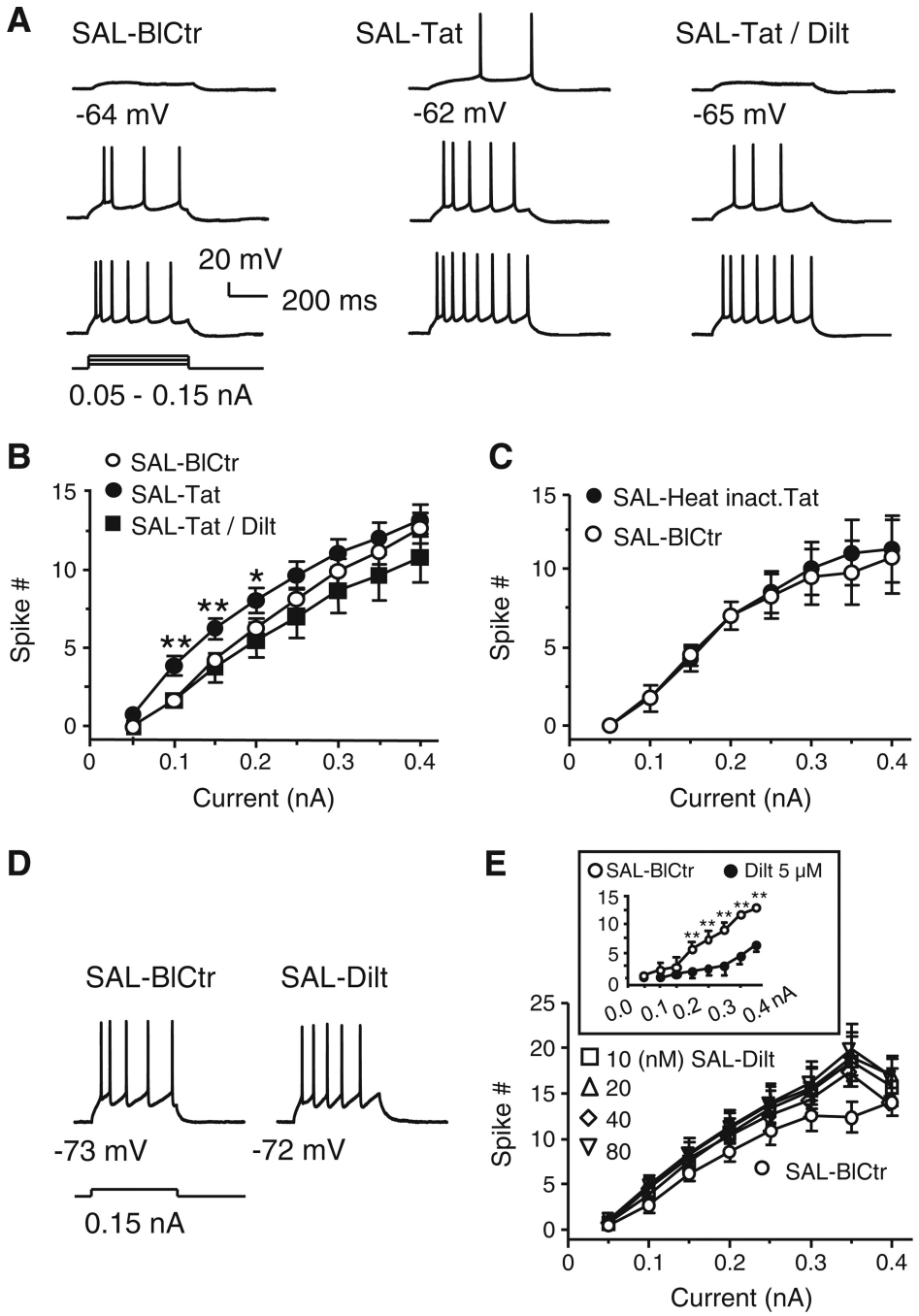

Fig. 1. Tat facilitated evoked firing; this effect was abolished by blocking L-type Ca^{2+} channels

All recordings were done in mPFC pyramidal neurons in forebrain slices obtained from SAL-treated rats. *Abbreviations* (used for all figures): SAL, saline-treated rats; BlCtr, baseline control recordings taken prior to *in vitro* bath-applied treatments; Tat, bath-applied Tat; Heat inact. Tat, Tat inactivated by heating and then bath applied; Dilt, bath-applied diltiazem; Tat/Dilt, Tat and diltiazem co-perfusion. ***a***. Recording traces from a single neuron illustrating that bath application of recombinant Tat (40 nM) increased evoked action potentials and this effect was blocked by co-perfusion with Dilt (40 nM). ***b***. Current-

response curves showing that Tat significantly increased the number of spikes evoked by depolarizing current pulses (n=8 neurons/8 rats; two-way rmANOVA, p=0.005; *post hoc* Newman-Keuls, *p<0.025, **p<0.01), and this effect was not seen during co-perfusion with Dilt (p>0.05). ***c***. Heat-inactivated Tat (40 nM) did not alter evoked firing (n=4 neurons recorded from 2 rats; two-way rmANOVA; p=0.605). ***d***. Traces from a single neuron illustrating that Dilt (40 nM) did not markedly affect evoked firing. ***e***. Concentration-response curves showing that 10, 20, 40, or 80 nM Dilt did not significantly alter evoked firing (n=7 neurons from 6 rats; two-way rmANOVA; p=0.418). Insert: A subset of neurons was also tested with 5 μM Dilt and this concentration was sufficient to reduce evoked firing (n=4 neurons from 3 rats; two-way rmANOVA with *post hoc* Newman-Keuls; ** p<0.01)

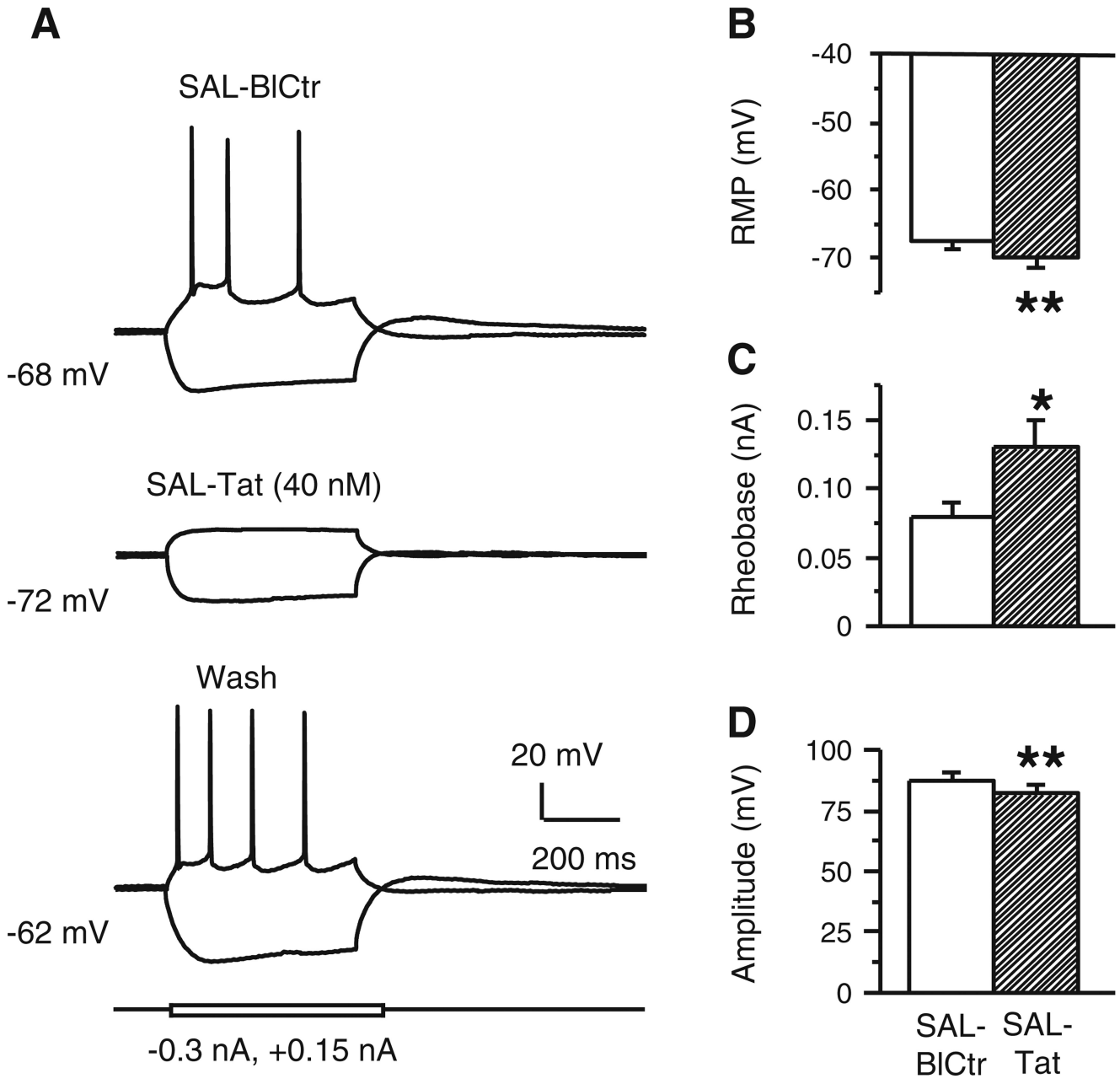

Fig. 2. Tat decreased evoked firing in some mPFC pyramidal neurons

a. Representative traces of a neurons recorded from a SAL-treated rat that showed reductions in spiking with bath applied 40 nM Tat (middle trace) that was reversed following 10–15 min of wash out (lower trace). ***b–d***. Associated with this decrease was a more hyperpolarized resting membrane potential (RMP), an increased rheobase, and a reduced spike amplitude (n=8 neurons recorded from 8 rats; paired *t*-test, **p*<0.05, ***p*<0.01)

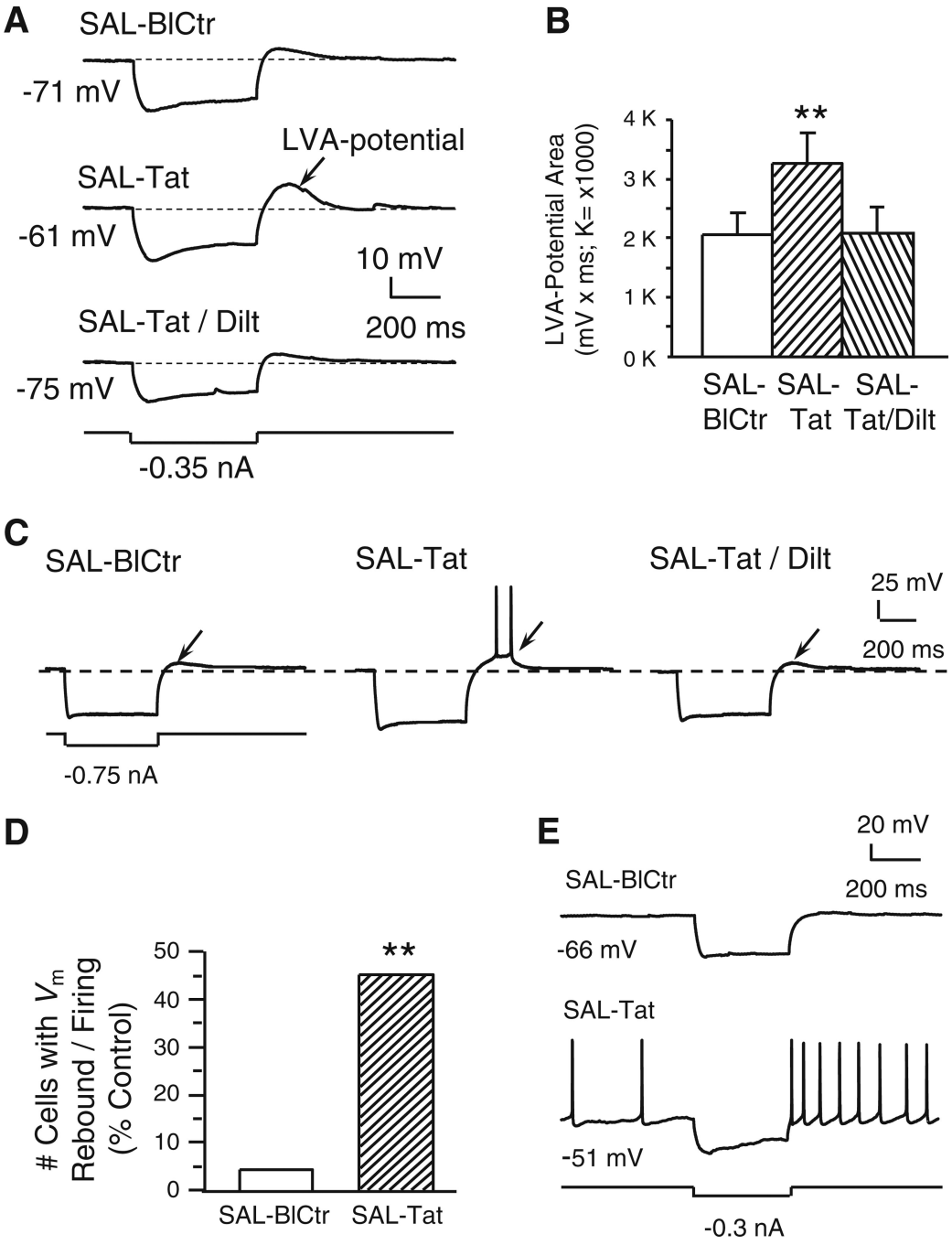

Fig. 3. Tat potentiated a subthreshold, low voltage-activated (LVA-) membrane potential and triggered spiking; both changes were abolished by diltiazem (indicated by arrows)

All recordings were in slices obtained from SAL-treated rats. ***a***. Recording traces illustrate that a marked membrane hyperpolarization (more negative than −110 mV) was immediately followed by a small, V_m rebound (i.e., a subthreshold, low voltage-activated (LVA)-potential; upper trace). Tat (40 nM) markedly enlarged this LVA potential (middle trace). The Tat-induced effect was abolished by concurrent bath application of diltiazem (40 nM; lower trace). ***b***. Quantification of LVA-potential area. Tat (40 nM) significantly enlarged the

subthreshold LVA-potential area and this effect was abolished by co-perfusion of diltiazem (40 nM) (n=9 neurons recorded from 9 rats; one-way rmANOVA, p=0.008; *post hoc* Dunnett's test, **p<0.01). ***c***. Traces from a single neuron illustrating that Tat-induced LVA-potential enhancement achieved the firing threshold and elicited spontaneous action potentials. ***d***. Number of neurons that displayed the LVA-potential and spontaneous firing triggered by the LVA-V_m rebound; data are presented as%of total neurons tested (n=22 from 17 rats). Only one neuron showed the V_m rebound-triggered firing prior to Tat perfusion. During Tat (40 nM) application, 10/22 neurons demonstrated V_m rebound-triggered firing (Chi-squared test, **p<0.01). ***e***. In two of the ten neurons showing the V_m rebound (illustrated are traces from one of these two), Tat (40 nM) depolarized the RMP to spiking threshold so that spontaneous firing occurred, and spiking was further enhanced by the V_m rebound in response to a hyperpolarizing stimulus

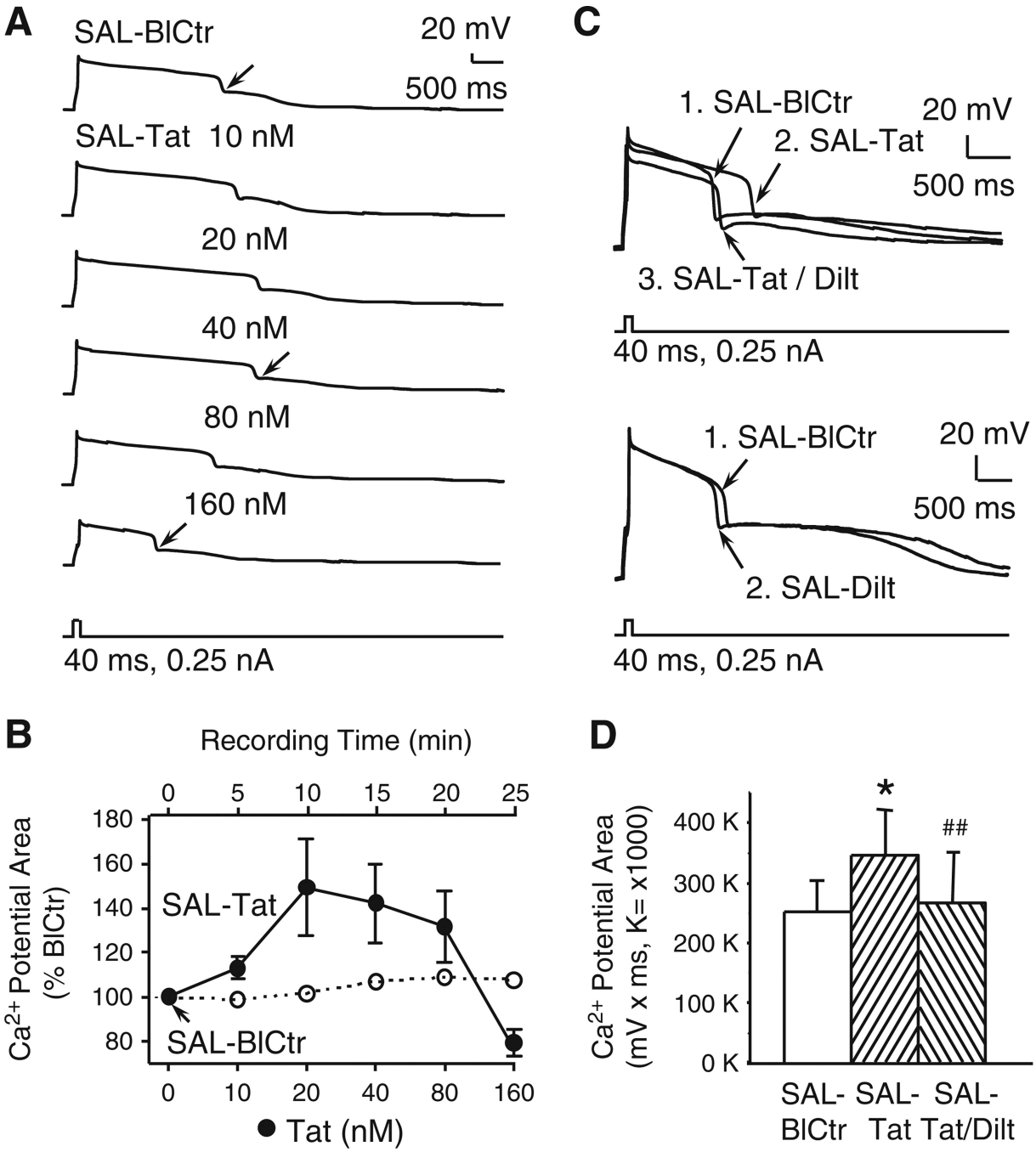

Fig. 4. Tat enhanced voltage-sensitive Ca^{2+} plateau potentials at lower concentrations, but decreases occurred at higher concentrations

All recordings were from slices obtained from SAL-treated rats. ***a***. Recording traces illustrating that lower concentrations (10–40 nM) of bath-applied Tat incrementally prolonged voltage-sensitive Ca^{2+} plateau potentials evoked by a depolarizing current pulse. Higher Tat concentrations (80, 160 nM) reduced the Ca2+ potentials. ***b***. Tat concentration-response relationship illustrating Tat (0–160 nM)-induced changes in evoked Ca^{2+} plateau potentials relative to pretreatment levels (i.e., % BlCtr; closed circles; 0–80 nM, n=7

neurons recorded from 7 rats; 160 nM, n=3 neurons from3 rats). For further qualitative comparison, the open circles show the responses of a representative pyramidal neuron recorded in the absence of Tat for the same period of time used for the concentration-response analysis (i.e., 25 min). Statistical evaluations of these recordings are included in the analyses for Fig. 6B. ***c***. Top illustration. Recording traces showing that Tat (40 nM) prolonged Ca^{2+} potential (trace #2 SAL-Tat *vs*. #1 SAL-BlCtr), and this enhancement was abolished by co-perfusion of diltiazem (20 nM) (trace #3 SAL-Tat/Dilt *vs*. #2 SAL-Tat). Bottom illustration. Diltiazem alone (40 nM) did not induce marked changes in the Ca^{2+} potential (trace #2 SAL-Dilt *vs*. #1 SAL-BlCtr). ***d***. Summary of recordings showing that the 40 nM Tat-induced increase in the Ca2+ potential area was blocked by co-perfusion of diltiazem (20 or 40 nM) (n=6 neurons from 6 rats, one-way rmANOVA, p=0.008; *post-hoc* Newman-Keuls; *p<0.05 compared to SAL-BlCtr, ##p<0.01 compared to SAL-Tat)

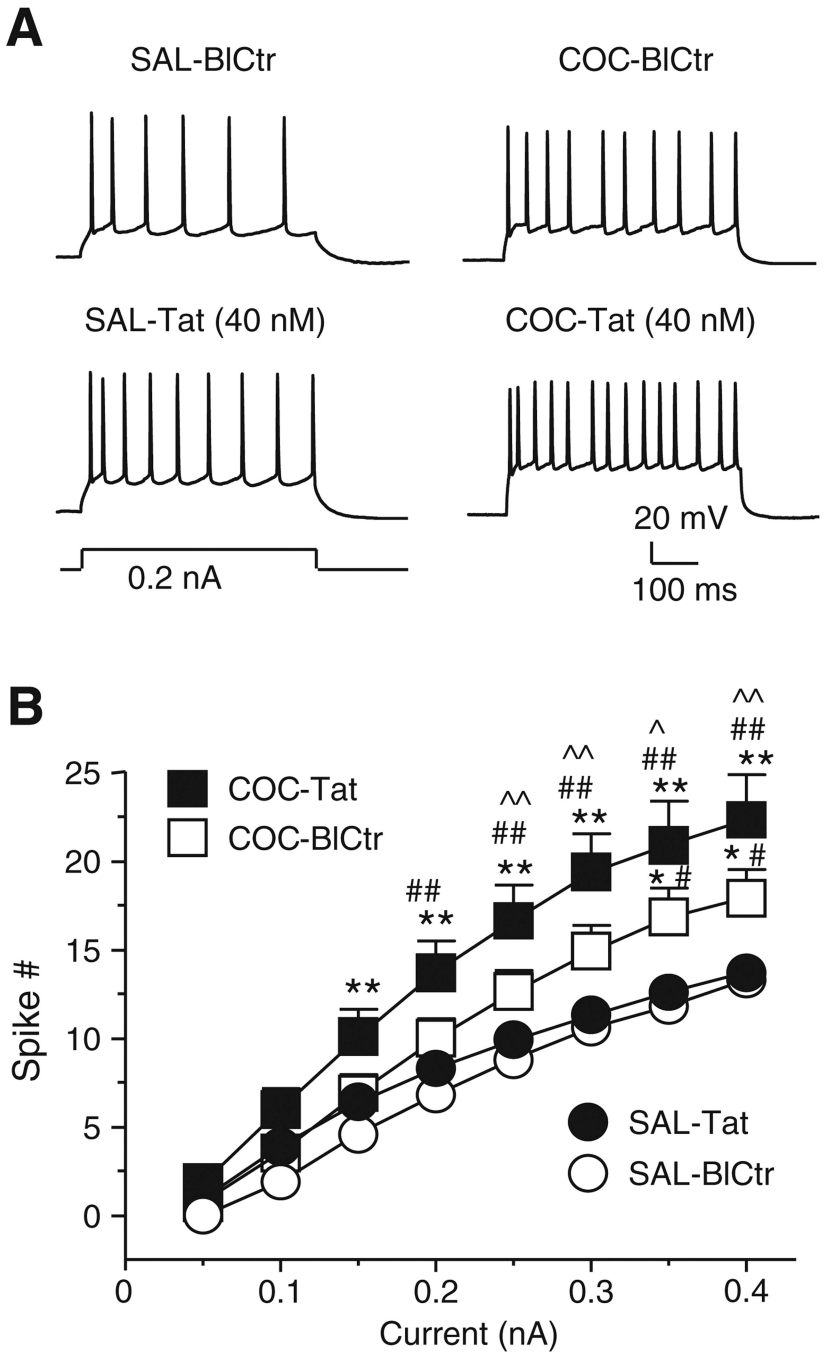

Fig. 5. Consequences of repeated cocaine administration on evoked firing before and during perfusion with Tat

a. Recording traces illustrating that the number of action potentials evoked by a moderate depolarizing current was markedly greater in a mPFC pyramidal neuron from a COC-treated rat (upper right trace) than that from a SAL-treated rat (upper left trace). Bath-applied Tat facilitated the evoked firing in both neurons (lower traces). ***b***. Relationship between the stimulation current magnitude and the number of evoked spikes during the following treatment conditions: SAL-BlCtr and SAL-Tat (n=10 neurons from 10 rats), COC-BlCtr and

COC-Tat (n=11 neurons from 5 rats). There was a significant difference in the effects of treatment, current, and interaction among the neurons with different treatments (two-way rmANOVA, all $p<0.001$). The signes and vertical bars represent the mean±S.E.M., respectively, as indicated. Significant differences between treatment conditions using a *post hoc* Newman-Keuls are illustrated as follows: *$p<0.025$ and **$p<0.01$, compared to SAL-BlCtr; #$p<0.025$ and ##$p<0.01$, compared with SAL-Tat; ^$p<0.025$, compared to COC-BlCtr. SAL-BlCtr and SAL-Tat groups included some cells that were also used to determine the effects of Tat and diltiazem on evoked firing (see Fig. 1B). It is noteworthy, that in contrast to data presented in Fig.1B, the sample and analysis used here did not detect a significant difference for spiking evoked by 0.1–0.20 nA between SAL-Tat and SAL-BlCtr. Such difference in the statistic outcomes could be attributed to the assumption that the neurons were considered as independet groups with different treatment, although the neurons with SAL-BlCtr and SAL-Tat treatment were actually from the same group, as well as those from COC-BlCtr and COC-Tat group

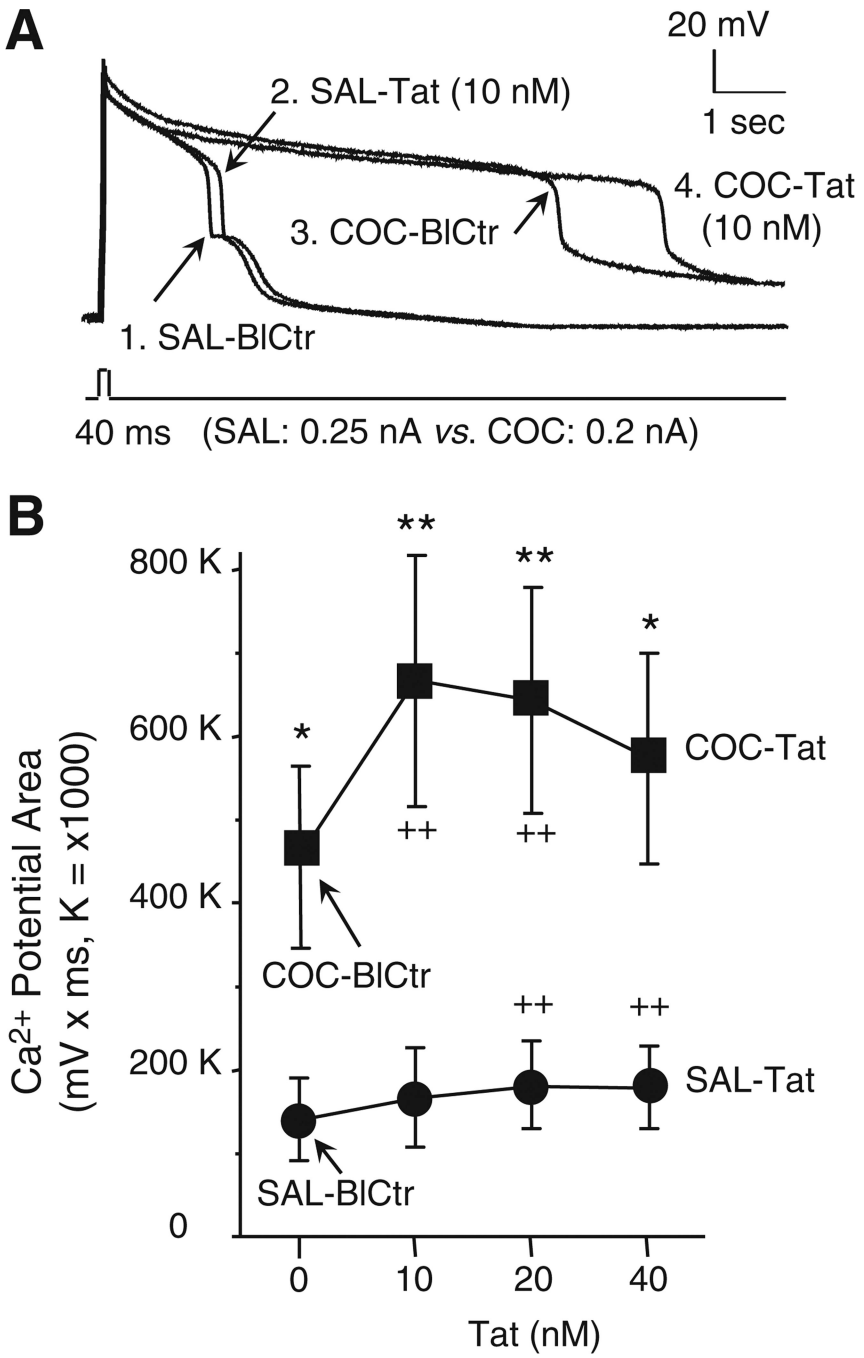

Fig. 6. Repeated cocaine enhanced Tat-induced increases in Ca^{2+} potentials

a. Recording traces from baseline (BlCtr) illustrating that the duration of Ca^{2+} potentials was remarkably prolonged in a mPFC pyramidal neuron from a COC-treated rat as compared to that from a SAL-treated rat (trace #3 COC-BlCtr *vs*. #1 SAL-BlCtr). A low concentration of bath-applied Tat (10 nM) induced an additional increase in the Ca^{2+} potential duration in a neuron from a COC-treated rat (trace #4 COC-Tat *vs*. #3 COC-BlCtr), the magnitude of which was greater than that recorded from a SAL-treated rat (trace #2 SAL-Tat *vs*. #1 SAL-BlCtr). Note: The rheobase (i.e., the current used to evoked these

potentials) for the neuron from the COC-treated rat was slightly lower than that from the SAL-treated rat (0.2 and 0.25 nA, respectively). ***b***. Concentration-response relationships illustrating the effects of bath-applied Tat (10–40 nM) on the integrated Ca^{2+} potential area in neurons from both SAL-treated (n=8 neurons from 8 rats; filled circles) and COC-treated (n=9 neurons from 6 rats; filled squares) rats. There was a significant difference in the effects of treatment, Tat concentration, and an interaction on the area of evoked Ca^{2+} potentials (two-way rmANOVA, p=0.013, <0.001, 0.004, respectively; the signs and vertical bars represent the mean±S.E.M., respectively). A *post hoc* Newman-Keuls test indicated that there was a significant difference in the Ca^{2+} potential area between the neurons from SAL-treated and COC-treated rats at baseline (0 nM) and 10–40 nM Tat (*p<0.05, **p<0.01). To assess the effects of Tat concentration, independent from the treatment of SAL or COC, a simple main effect analysis (one-way rmANOVA) with *post hoc* Dunnett's was used. In the neurons from SAL-treated rats, bath-applied Tat (i.e., SAL-Tat) significantly increased the Ca^{2+} potential area at 20 and 40 nM compared to SAL-BlCtr (++p<0.01). In the neurons from COC-treated rats, the Ca^{2+} potential area reached its maximum level with perfusion of Tat at 10 nM as compared to the COC-BlCtr (p=0.006; with *post hoc* Dunnett's test, ++p<0.01). There was no significant difference in the Ca^{2+} potential area between COC-Tat (40 nM) and COC-BlCtr (p>0.05), consistent with response blunting per 'overactivation'. It is worth noting that a subthreshold concentration of Tat (10 nM), which did not induce a significant increase in Ca^{2+} influx in the neurons from SAL-treated rats, enhanced Ca^{2+} influx to the level which was greater than the additive effects of acute Tat and chronic COC without Tat, This suggested that there might be a synergistic effect of cocaine and Tat. The signes and vertical bars represent the mean±S.E.M., respectively

Table 1

Effects of acute *in vitro* application of 40 nM Tat and chronic *in vivo* exposure of cocaine on the membrane properties of rat mPFC pyramidal neurons that showed Tat-induced increases in spiking

	SAL-BlCtr	SAL-Tat	COC-BlCtr	COC-Tat
No. Neurons (No. Rats)	10 (10)	10 (10)	11 (5)	11 (5)
RMP (mV)	−67.8±1.3	−65.5±1.5**	−67.0±1.6	−64.9±1.6^{+}
R_{in} (MΩ)	192±26	236±24*	206±17	264±28^{++}
Rheobase (nA)	0.11±0.01	0.07±0.01**	0.08±0.01*	0.06±0.01^{+}
Threshold (mV)	−42.3±1.3	−42.5±1.3	−41.5±1.0	−38.4±2.2
½ Peak Duration (ms)	2.1±0.2	2.1±0.2	1.7±0.2	2.5±0.5^{++}
Amplitude (mV)	90.3±5.0	83.2±5.5*	74.6±3.9*	59.1±2.7$^{++,\#\#}$
AHP (mV)	8.5±1.5	7.9±1.4	12.4±1.3	8.6±0.8

Two-way rmANOVA:
RMP: acute Tat, $F_{(1,19)}$=19.893, p<0.001; chronic cocaine, $F_{(1,19)}$=0.042, p=0.840; Interaction, $F_{(1,19)}$=0.359, p=0.556
R_{in}: acute Tat, $F_{(1,19)}$=16.946, p<0.001; chronic cocaine, $F_{(1,19)}$=0.419, p=0.525; Interaction, $F_{(1,19)}$=0.236, p=0.633
Rheobase: acute Tat, $F_{(1,19)}$=38.214, p<0.001; chronic cocaine, $F_{(1,19)}$=1.418, p=0.248; Interaction, $F_{(1,19)}$=10.933, p=0.004
Threshold: acute Tat, $F_{(1,19)}$=1.195, p=0.288; chronic cocaine, $F_{(1,19)}$=2.099, p=0.164; Interaction, $F_{(1,19)}$=1.424, p=0.247
½ peak duration: acute Tat, $F_{(1,19)}$=5.670, p=0.028; chronic cocaine, $F_{(1,19)}$=0.001, p=0.984; Interaction, $F_{(1,19)}$=5.384, p=0.032
AP amplitude: acute Tat, $F_{(1,19)}$=10.350, p=0.005; chronic cocaine, $F_{(1,19)}$=12.500, p=0.002; Interaction, $F_{(1,19)}$=7.665, p=0.014
AHP: acute Tat, $F_{(1,19)}$=1.570, p=0.225; chronic cocaine, $F_{(1,19)}$=0.640, p=0.434; Interaction, $F_{(1,19)}$=0.997, p=0.331

post hoc Newman-Keuls:

$^{*}p$<0.05

$^{**}p$<0.01; *vs.* SAL-BlCtr

^{+}p<0.05

^{++}p<0.01; *vs.*COC-BlCtr

$^{\#\#}p$<0.01; *vs.* SAL-Tat